

# Ultrafast carrier localisation in the pseudogap state of cuprate superconductors from coherent quench experiments.

I.Madan<sup>1</sup>, T.Kurosawa<sup>2</sup>, Y.Toda<sup>3</sup>, M.Oda<sup>2</sup>, T.Mertelj<sup>1</sup>, D.Mihailovic<sup>1</sup>

<sup>1</sup>Jozef Stefan Institute and International Postgraduate School, Jamova 39, SI-1000 Ljubljana, Slovenia

<sup>2</sup>Department of Physics, Hokkaido University, Sapporo 060-0810, Japan and

<sup>3</sup>Department of Applied Physics, Hokkaido University, Sapporo 060-8628, Japan

A “pseudogap” (PG) was introduced by Mott to describe a state of matter which has a minimum in the density of states at the Fermi level, deep enough for states to become localized. It can arise either from Coulomb repulsion between electrons, or due to an incipient charge or spin order, or a combination of the two. These states are rapidly fluctuating in time with random phase, so they are hard to observe experimentally. Here we present the first coherent quench measurements of the dynamical transition to the pseudogap state in the prototype high temperature superconductor  $\text{Bi}_2\text{Sr}_2\text{CaCu}_2\text{O}_{8+\delta}$ , revealing a marked absence of incipient collective ordering beyond a few coherence lengths on short timescales at any level of doping. Instead we find evidence for sub-picosecond carrier localization favouring a picture of pairing resulting from the competing Coulomb interaction and strain, enhanced by a Fermi surface instability.

A “pseudogap” (PG) was introduced by Mott to describe a state of matter which has a minimum in the density of states at the Fermi level, which is deep enough for the states to become localized<sup>1</sup>. It results either from Coulomb repulsion between electrons on the same atom, a bandgap in a disordered material or a combination of both. The PG appears in many different systems under current investigation, and is of ever increasing interest<sup>2–4</sup>, partly due to the resulting unusual physical properties, and partly because it is commonly associated with the emergence of a long-range ordered broken symmetry state, such as superconductivity (SC) or a charge or spin density wave order.<sup>5</sup> Understanding its origin in the particular case of high-temperature superconductors is thought to be of primary importance for determining the mechanism for the formation of high-temperature superconductivity. In the absence of evidence for any phase transitions associated with the PG state, either fluctuating charge-density wave (CDW) or stripe electronic order has recently been favoured as the origin of the PG state in the cuprate superconductors<sup>6,7</sup>. The collective nature of a CDW state would imply critical slowing down associated with the onset of long range order in the dynamical phase transition, which would not necessarily be present in the case of stripes. Here we report on experiments specifically designed to detect critical behavior associated with the appearance of the PG state in a non-equilibrium transition with femtosecond coherent control experiments. The method allows us to either confirm or exclude the existence of long-range charge or spin order on short timescales and allows us to estimate the correlation length of the ordered state. Our experiments on a prototype cuprate  $\text{Bi}_2\text{Sr}_2\text{CaCu}_2\text{O}_{8+\delta}$  (Bi-2212) in different regions of the phase diagram show a clear *absence* of divergence of the single particle relaxation time coincident with the emergence of pseudogap state, thus excluding the presence of collective order beyond a few superconducting coherence lengths. The emerging physi-

cal picture for the origin of the pseudogap is Mott-like carrier localisation and aggregation into short stripes, rather than incipient dynamic or fluctuating charge density wave order.

From experiments so far, it is clear that the appearance of the PG state in the cuprates is not related to a classical thermodynamic transition, and no signatures of latent heat or anomalies are observed in the heat capacity temperature dependence.<sup>8</sup> However, its gradual appearance below a certain temperature  $T^*$  is detected by numerous techniques.<sup>2,5,9</sup> The observed effects are consistent with a depression of the density of states at the Fermi energy below this temperature. Recently a more specific origin for the appearance of fluctuating charge density wave order was discussed<sup>10</sup> as an alternative to carrier localization in the form of polarons (or clusters of polarons)<sup>11,12</sup>, where the origin of the PG in the former case is related to the formation of a periodic potential opening a gap in the low energy spectrum, while in the latter, the energy scale associated with the PG is related to the binding energy of the localized states. The apparent correlation between the appearance of the PG and stripe order has been intensively discussed for some time<sup>13–15</sup>, and recently reinvigorated<sup>6,7,10,16,17</sup>, opening further questions regarding the relation of stripes with charge density wave order.

In high-temperature superconducting cuprates, the pseudogap was often thought to be a precursor rather than a competitor of the SC state. An apparent 4-fold symmetry of the PG state is compatible with a  $d$ -wave SC state symmetry observed by ARPES<sup>18</sup> and STS<sup>19</sup>. It was however shown that pseudogap does not evolve into the superconducting gap, but rather coexists with it<sup>8,20–25</sup>. It was further shown that the PG temperature  $T^*$  is quite distinct from the onset of superconducting fluctuations<sup>26–30</sup>. One similarity which the pseudogap state shares with superconductivity from the point of view of time-resolved

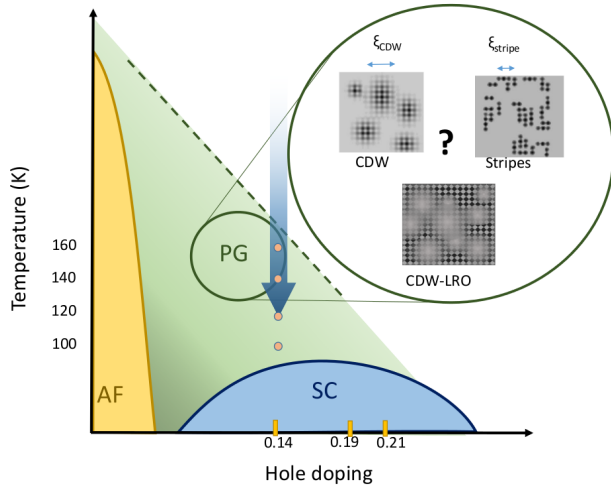


Figure 1. **Phase diagram.** A phase diagram highlighting the different candidates most often discussed for the PG state: a) a CDW-like state with spatial phase and amplitude fluctuations, b) a stripe-like order arising from competing interactions, or c) a long-range ordered (LRO) macroscopically coherent state with spatial amplitude fluctuations. The arrow shows the quench path. The orange dots schematically represent the base temperatures at which the data are measured. The doping level corresponding to the three samples investigated here is also shown.

optical experiments is that in both cases gaps can be destroyed by an ultrashort laser pulse<sup>31,32</sup>. This fact is especially intriguing, because there is no signatures of condensation energy associated with the pseudogap observed in the heat capacity measurements<sup>8</sup>.

In Bi-2212 the observed charge modulation is incommensurate and has  $\sim 4a \times 4a$  periodicity<sup>33</sup> and its onset seems to correlate with the pseudogap temperature  $T^*$ <sup>6,7</sup>. Although pinned in STM measurements, charge order is often thought to be fluctuating<sup>10</sup> and consequently should be characterizable by ultrafast techniques. Whether the pseudogap is associated with an order parameter characterizing a collective state with long range order, defined at least on the ultrafast time scale, or is a stripe-like state of aggregated localized particles is an important open question (see Fig.1).

Recent pump-probe experiments measuring the coherent electronic Raman response have shown broken rotational symmetry associated with the appearance of the pseudogap state in Bi-2212.<sup>34</sup> The pseudogap response has been identified in the  $B_{2g}$  symmetry channel of the parent  $D_{4h}$  point group. However these experiments did not reveal any characteristic length scale or the origin of the PG excitation - so it was not clear whether the broken symmetry state is long-range ordered or symmetry is broken only locally by objects such as polarons. The experiments also did not show whether the symmetry breaking is static or dynamic.

In gapped laser-excited systems evolving through a tran-

sition *in time*, critical behavior is displayed by the quasi-particle (QP) lifetime  $\tau_{QP}$  which is approximately inversely proportional to the gap  $\Delta$  in the vicinity of the critical time  $t_c$  of the transition. This behaviour is ubiquitous and has been seen in both superconducting and charge-density wave systems appearing as an unmistakable divergence of the QP lifetime at  $t_c$ , concurrent with the appearance of a QP gap. Examples from 3-pulse coherent control experiments include both quasi-1D and quasi-2D systems: TbTe<sub>3</sub>, DyTe<sub>3</sub>, 2H-TaSe<sub>2</sub>, K<sub>0.3</sub>MoO<sub>3</sub><sup>35</sup> and superconducting La<sub>2-x</sub>Sr<sub>x</sub>CuO<sub>4</sub>.<sup>36</sup> The QP lifetime divergences associated with the superconducting transition are observed ubiquitously in cuprates (YBCO<sup>25</sup>, LSCO<sup>37</sup>, BiSCO<sup>31</sup>, Hg<sup>38</sup>, YBCO124<sup>39</sup> and pnictides<sup>40</sup>. A similar divergence is also observed at the SDW transition in pnictides<sup>41,42</sup>.

It is important to emphasize the principal difference of behaviour of *non-homogeneous systems* in quasi-ergodic slow-cooling experiments and phase transitions in coherently excited rapid quench experiments where the elementary excitations may be both highly out of equilibrium amongst themselves and also spatially inhomogeneous.

Particularly we would like to highlight the difference between the single particle relaxation time in slow cooling experiments compared with a system freely evolving in time through a gap-forming transition. When a system is slowly cooled through the critical temperature, a gap appears in different regions at different  $T$ , and critical behavior is smeared out and becomes undetectable. On the other hand when a rapid quench occurs in an inhomogeneous system, a gap starts to appear simultaneously throughout the whole sample volume and critical behaviour is still observed close to the transition, albeit with a non exponential relaxation. Thus even if the QP lifetimes are different in different regions of the sample, a signal revealing critical slowing down will still be observable. This subtle, but important difference allows us to search for QP lifetime divergence in the time-resolved optical reflectivity which would signify the presence of charge order on all relevant time-scales down to a few tens of fs. The condition for a coherent response is that the excitation time  $\tau_{ex}$  is shorter than the time it takes for the PG state to form, i.e. the PG recovery time  $\tau_{rec}$ .  $\tau_{ex}$  is determined by the energy relaxation time  $\tau_E \simeq 50$  fs<sup>43</sup>, while here we will show  $\tau_{rec} \simeq 600$  fs, so this condition is fulfilled. The experiments can thus either conclusively confirm or categorically exclude the presence of long-range order and thus distinguish between the different PG states shown in Fig. 1 and also enable us to estimate the effective correlation lengths of PG excitations.

## RESULTS

The photoinduced reflectivity ( $\Delta R/R$ ) below  $T^*$  in Bi-2212 ubiquitously shows two relaxation components

(Fig. 2a)). One is the PG response (which appears as photoinduced decrease in reflectance) and the other arises from hot electrons energy relaxation (and appears as an increase in reflectance)<sup>31,44</sup>. With increasing fluence  $\mathcal{F}$  both components initially increase linearly, followed by a saturation of the negative PG component. The energy relaxation component remains linear with  $\mathcal{F}$  for all measured fluences and does not change significantly with temperature<sup>31</sup>, so it can be easily subtracted to obtain only the PG signal. The saturation of the PG response was shown to be associated with the photodestruction of the PG state<sup>31</sup> which is clearly nonthermal, since the estimated lattice temperature rise due to the laser excitation is  $< 6$  K.

In Fig. 2d) and e) we plot normalized fluence dependence of the amplitude of the PG response for different temperatures and dopings respectively. For an accurate quantitative analysis of the fluence dependence and estimation of the threshold fluence (the point of departure from  $\mathcal{F}$ -linear behavior) we take into account the inhomogeneous excitation due to the finite light penetration depth<sup>45</sup>. Fits are represented as solid lines in Fig. 2d) and e).

As shown in Fig. 1d) the fluence behavior nicely scales for different temperatures indicating that the PG photodestruction threshold fluence is apparently temperature independent. The value of  $\Delta R/R$  at saturation falls with increasing temperature (shown in black squares in Fig. 2b)) and follows the T-dependence of the pseudogap response in weak excitation regime (open circles in Fig. 2b)). In Fig. 2e) we plot the fluence dependence of the pseudogap response amplitude for the three different doping levels. The fluence dependence is very similar for all doping levels, differing only in the threshold value which increases monotonically with  $T^*$  and accordingly decreases with doping ( Fig. 2c)).

The time evolution of the PG response through the transition measured in the three pulse experiment is shown in Fig. 3. First, we note that the *hot electron energy relaxation response* remains unaffected by the D pulse, (also at room temperature, i.e. above  $T^*$ ), and we can thus subtract it in all further data analysis. The pump induced *pseudogap response* is suppressed at the moment when the D pulse arrives (shown by the dashed line). At later delays  $t_{D-P}$  we observe reappearance of the negative PG response. In the inset of Fig. 4 we plot the magnitude of the PG signal after the subtraction of the positive component, measured at the room temperature. The relaxation times obtained from the fit to the data in the inset of Fig. 4 are shown in Fig. 4. Within experimental error, the PG relaxation time is constant throughout the PG recovery, at  $\tau_{PG} = 0.26 \pm 0.05$  ps. Remarkably, and in contrast to established behavior in CDW<sup>35</sup> and superconducting<sup>36</sup> systems investigated so far, no critical behavior of the SP response is observed close to  $t_c$ , the critical time of the transition. This observation has important implications with regards to the possible collective nature of the pseudogap state. We emphasize that

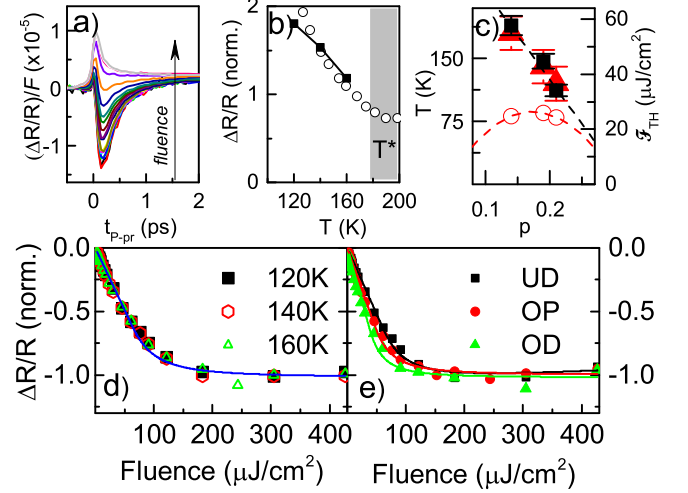


Figure 2. **Pseudogap response as a function of fluence.** a) Transient reflectivity normalized by the incident fluence  $(\Delta R/R)/\mathcal{F}$  for underdoped sample at 120K. At low excitation the response is linear and curves overlap. At low excitation negative pseudogap component is dominant, whereas at high excitation it is saturated and hot-electron energy relaxation component is prevailing. b) Amplitude of the saturated pseudogap signal  $(\Delta R_{SAT}/R)$  as a function of temperature (black squares). For comparison renormalized low fluence temperature dependence of the amplitude from<sup>31</sup> is plotted (open circles) c) The value of photodestruction threshold fluence (black squares) as a function of doping. For comparison doping dependence of  $T^*$  (red triangles) and  $T_c$  (red circles) are shown in the same graph. d) Normalized fluence dependence of the amplitude of the pseudogap component at different temperatures for the underdoped sample. e) Normalized fluence dependence of the amplitude of the pseudogap component for different doping levels: underdoped (UD) at 120 K, optimally doped (OP) at 120 K and overdoped (OD) at 110 K.

the observation of the absence of critical slowing down at early recovery time is different from its absence in temperature scans: for possibly inhomogeneous sample in the case of the temperature dependence at some defined temperature  $T_1$  only regions of the sample with this particular  $T^* = T_1$  would show critical slowing down of SP relaxation, whereas in the quenched case the onset of the pseudogap, and consequently the critical slowing down, is simultaneous throughout the destruction region. The absence of divergence might indicate that the normal to pseudogap transition is of first order. However, in this case we expect to observe an obvious change of relaxation time at  $T^*$ <sup>46</sup>. Such effect has not been observed, so a first order transition can be ruled out.

To compare the dynamics of the pseudogap recovery at different destruction fluences we plot in Fig. 5 normalized amplitude of the pseudogap component as a function of  $t_{D-P}$ , at different temperatures. Within the accuracy of the measurement the PG recovery time  $\tau_{rec}$  is virtually

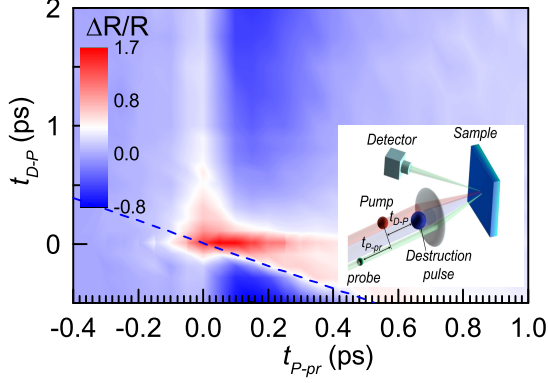


Figure 3. **Typical result of the three pulse experiment.** Underdoped sample at 120 K, the D pulse fluence is  $204 \mu\text{J}/\text{cm}^2$ . The time of the D pulse arrival is shown by the dashed line. The D pulse suppresses the negative pseudogap component, whereas the hot electron energy relaxation response remains intact. Note that at later  $t_{D-P}$  the positive component is masked by the stronger negative PG component with a slower rise time. The inset shows a schematic picture of the three-pulse pump-probe experiment with the sequence of pulses and notation of delays. Colors of the pulses do not correspond to their photon energy.

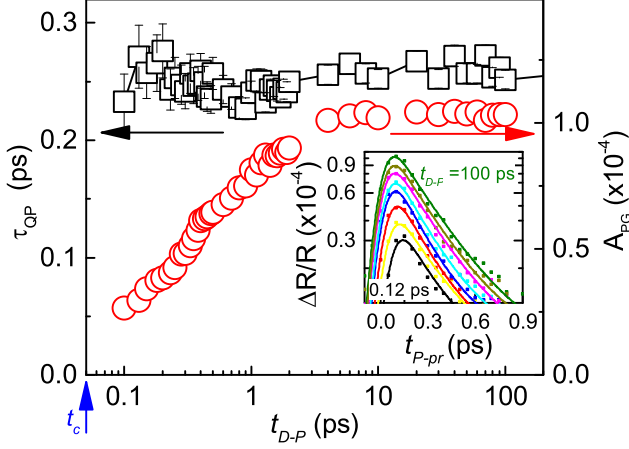


Figure 4. **Evolution of amplitude and QP relaxation time.** Quasiparticle relaxation time (black dots, left axis) and the amplitude (red open circles, right axis) of the pseudogap component (data shown in inset) as a function of  $t_{D-P}$ . Quasiparticle relaxation time remains constant for all values of  $t_{D-P}$ . Inset: Pseudogap component for different values of  $t_{D-P}$  ( $\mathcal{F} = 204 \mu\text{J}/\text{cm}^2$ ,  $T = 120\text{K}$ ).

fluence independent. Remarkably, for all temperatures and fluences, the PG recovery shown in Fig. 5 can be fit with an exponential function, which is not the case in the recovery of SC and CDW orders, where the dynamical recovery behavior associated with the formation of a collective state is more complicated. Such a simple expo-

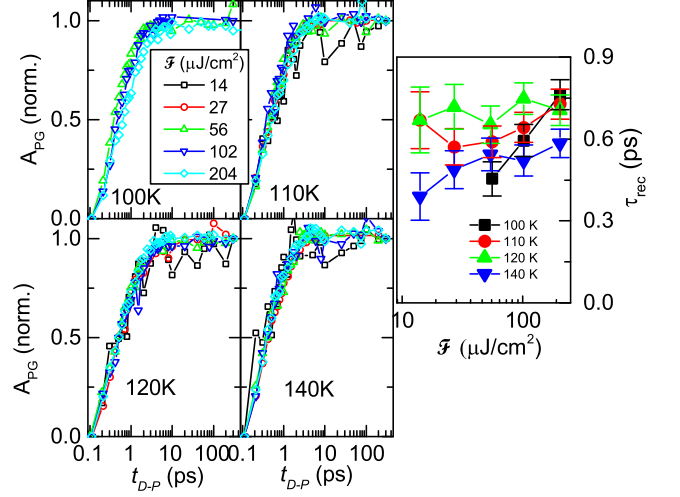


Figure 5. **Recovery of the PG state after destruction by a laser pulse as a function of fluence at different temperatures.** The normalized amplitude of the pseudogap component as a function of  $t_{D-P}$  for different fluences at a number of temperatures is plotted. Inset: the recovery time  $\tau_{rec}$  as a function of fluence  $\mathcal{F}$  at different temperatures.

nential recovery is consistent with uncorrelated dynamics of independent particles.

## DISCUSSION

The distinct absence of critical behavior as  $t \rightarrow t_c$  in the PG state gives us new insight into the mechanisms for its formation. The absence of a divergence in the SP excitation dynamics is a signature of finite size of the system either limited externally or just indicating a local nature of the excitation. The 50 fs uncertainty of the measured value of  $\tau_{QP}$  allows us to put an upper limit on the correlation size of the pseudogap excitation. Taking the Fermi velocity as a maximum fluctuations propagation speed of  $v_F \sim 150 \text{ nm/ps}$ <sup>47</sup> we obtain  $\xi_{cor}^{max} \sim 75 \text{ \AA}$  which is only a few superconducting coherence lengths, and indicates a rather local nature of the PG state.

A number of experiments suggest that the pseudogap is associated with bound (or localized) states<sup>16,48–52</sup>. A simple but plausible picture<sup>25</sup> is that photoexcitation leads to the excitation of carriers from these states into itinerant states. Thereafter binding takes place on a timescale given by  $\tau_{rec}$  which is nearly independent on fluence and temperature, again suggesting non-collective behavior. This picture is supported by the fact that the pseudogap is *filled rather than destroyed* (i.e. *closed*) after photoexcitation<sup>53</sup>, i.e. a number of delocalized “in-gap states appear” without strongly altering the binding energy. This is tantamount to saying that the states do



not act cooperatively, and there is no change of the energy scale, as the system evolves through  $t_c$  in time.

In the analysis of the fluence dependence [Fig. 1d) and e)] we have used a model which assumes that the photoinduced absorption is proportional to the density of photoinduced quasiparticles. This is in turn linear with excitation intensity. This model has been shown to give a good description of superconducting condensate destruction, where the number of particles in the condensate is final<sup>45</sup>. In the case of the pseudogap with localized excitations, the simplest way to describe the state is in terms of a two-level system (TLS), in which case the expected  $\mathcal{F}$  dependence might be different. If photoexcitation directly excites particles from the ground state into the excited state the behaviour as a function of fluence would be described by saturation of the excited state population  $\sim \mathcal{F}/(1 + \mathcal{F}/\mathcal{F}_0)$ , where only half of the localized particles are excited at high intensities. However, 1.5 eV photons do not excite particles across the TLS directly, but create large numbers of electrons and holes through avalanche multiplication associated with hot carrier energy relaxation which then populate the excited state and deplete the ground state (filled with holes). If the hot electron energy relaxation time  $\tau_{e-ph} \lesssim 50$  fs<sup>43,54</sup> is shorter than the excited state relaxation time  $\tau_{PG} \simeq 260$  fs, then a bottleneck is formed, and we revert to the same scenario for the saturation of the photoexcited response as for the superconducting condensate. Additional confirmation that localized carriers are not excited directly by pump photons, but rather as a result of the avalanche process is that the pseudogap component is slightly delayed with respect to the hot electron relaxation response - see Fig. 3 (the positive component precedes the negative component).

Within this model, the photodestruction fluence threshold  $\mathcal{F}_{TH}$  is proportional to the density of bound carriers and inversely proportional to the photoexcitation efficiency which is defined as a ratio of energy spent on quasiparticle excitation to the total absorbed photon energy. The number of states involved in pseudogap formation can be estimated from electronic heat capacity and has been shown to decrease with doping<sup>8</sup> which explains the proportionality  $\mathcal{F}_{TH} \sim \Delta$  shown in Fig. 2 c). The apparent independence of the photodestruction fluence on temperature can be explained by relative inefficiency of thermal excitation from localized states at the temperature of the measurements, so that number of photoexcited carriers is an order of magnitude larger than thermally excited. Estimated  $\lesssim 3\%$  difference in photodestruction energy due to the distinction in the number of bound carriers at highest and lowest temperatures of the measurements is within the  $\sim 6\%$  error of our experiment.

Regarding the origin of the localization, while CDW patches<sup>10</sup> and mesoscopic stripes are sometimes confused, and may appear to be similar in some experimental observations, their implied origin is different. In the former case, the CDW and accompanying translational symme-

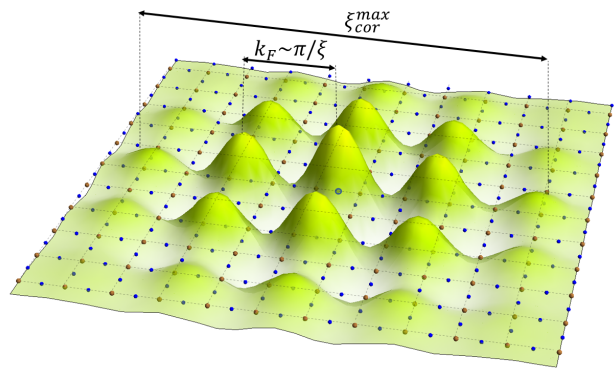


Figure 6. The real-space charge density map corresponding to a short-range Friedel oscillation around a localised carrier arising from an enhanced pairing susceptibility at inter-particle distances of  $k_F \sim \pi/\xi$ . The correlation length  $\xi_{corr}^{max}$  from the present experiments is also shown.

try breaking is caused by the Fermi surface (FS) physics, such as nesting at specific wavevectors leading to a FS instability. Recent ARPES studies have revealed that the wavevector of modulation does not correspond to the nesting between parallel sheets of FS at the antinodes but rather to the vector connecting “endpoints” of “Fermi arcs”, so no “true” nesting takes place.<sup>6</sup> Mesoscopic stripe textures on the other hand are usually considered within the strong coupling picture to be a result of the competing interactions, such as microscopic strain caused by localised holes and the Coulomb repulsion between them,<sup>11,12,55–57</sup> or the hole kinetic energy competing with the Coulomb interaction within Hubbard or  $t-J$  models<sup>58–61</sup>. However, these models per-se do not address the large variation in  $T_c$ s observed in the cuprates. Although not directly responsible for CDW formation, even a weak FS instability may act to additionally stabilize hole pairs within the strongly correlated picture discussed above. This adds an additional material-specific component which has a direct effect on  $T_c$ , namely the degree of nesting of the states at the Fermi surface<sup>18</sup>. This enhancement is not necessarily static: short stripe segments may form as dynamically fluctuating Friedel oscillations around localised carriers (Fig. 6). Indeed, the  $q$ -vector observed in X-ray experiments corresponds closely with the  $q$ -vector of the lattice and spin anomalies observed by inelastic neutron scattering experiments in  $\text{YBa}_2\text{Cu}_3\text{O}_{7-\delta}$  (<sup>62–64</sup>). Such a mechanism would have an effect in enhancing the pair stability in the antinodal directions (along the Cu-O bonds), and hence raising  $T_c$ .

To conclude, the data presented here, particularly the behaviour of the PG relaxation time through the coherently excited dynamical transition in Fig. 4 imply a picture where the pseudogap state is characterized by a short-range correlated localized carriers, pairs or very small clusters, locally breaking rotational symmetry<sup>34</sup>, rather than proper charge density wave segments (Fig. 1) discussed in the  $\text{LaSrCuO}$  system away from  $1/8$  doping.<sup>10</sup>

The observations are thus more consistent with a polaronic picture than a dynamically fluctuating charge density wave with long range order. Our experiments also clearly show that the character of the PG state does not change with doping in Bi2212. Only the energy associated for its destruction diminishes with increasing doping, reflecting the change of localisation energy (and  $T^*$ ) with increasing screening.

## METHODS

The pulse train of 50 fs 800 nm laser pulses from a Ti:Sapphire regenerative amplifier with a 250-KHz repetition rate was used to perform pump-probe (P-pr) reflectivity measurements. For the three pulse experiment each laser pulse was split in three: the strongest destruction (D) pulse was used to destroy the state while the

evolution of the state was monitored by measuring the pump-probe response at different delays between the D and P pulse.

Three samples with different doping levels were investigated in this work: under- ( $T_c = 81$  K,  $T^* = 180$  K), near optimally- ( $T_c = 85$  K,  $T^* = 140$  K) and over- ( $T_c = 80$  K,  $T^* = 120$  K) doped Bi2212 with hole concentrations  $p = 0.14, 0.19$  and  $0.21$  respectively. Samples were grown by the traveling solvent floating zone method. Their critical temperatures were obtained from susceptibility measurements, doping levels and pseudogap temperatures were estimated from previous studies<sup>65</sup>.

## Acknowledgments

Authors would like to thank Viktor Kabanov for valuable discussions.

- 
- <sup>1</sup> Mott, N. F. Metal-Insulator Transition. *Rev. Mod. Phys.* **40**, 677–683 (1968).
  - <sup>2</sup> Timusk, T. & Statt, B. The pseudogap in high-temperature superconductors: an experimental survey. *Rep. Prog. Phys.* **62**, 61–122 (1999).
  - <sup>3</sup> Sacépé, B. *et al.* Pseudogap in a thin film of a conventional superconductor. *Nat. Commun.* **1**, 140 (2010).
  - <sup>4</sup> Mannella, N. *et al.* Nodal quasiparticle in pseudogapped colossal magnetoresistive manganites. *Nature* **438**, 474–8 (2005).
  - <sup>5</sup> Norman, M. R., Pines, D. & Kallin, C. The pseudogap: friend or foe of high  $T_c$ ? *Adv. Phys.* **54**, 715–733 (2005).
  - <sup>6</sup> Comin, R. *et al.* Charge order driven by Fermi-arc instability in  $\text{Bi}_2\text{Sr}_{2-x}\text{La}_x\text{CuO}_{6+\delta}$ . *Science* **343**, 390–2 (2014).
  - <sup>7</sup> Parker, C. V. *et al.* Fluctuating stripes at the onset of the pseudogap in the high- $T_c$  superconductor  $\text{Bi}_2\text{Sr}_2\text{CaCu}_2\text{O}_{8+x}$ . *Nature* **468**, 677–80 (2010).
  - <sup>8</sup> Loram, J. W., Luo, J. L., Cooper, J., Liang, W. & Tallon, J. L. The condensation energy and pseudogap energy scale of Bi:2212 from Electronic specific heat. *Physica C* **348**, 831–834 (2000).
  - <sup>9</sup> Hufner, S., Hossain, M. a., Damascelli, A. & Sawatzky, G. a. Two gaps make a high-temperature superconductor? *Rep. Prog. Phys.* **71**, 062501 (2008).
  - <sup>10</sup> Torchinsky, D. H., Mahmood, F., Bollinger, A. T., Božović, I. & Gedik, N. Fluctuating charge-density waves in a cuprate superconductor. *Nature materials* **12**, 387–91 (2013).
  - <sup>11</sup> Alexandrov, A. S. & Mott, N. F. Bipolarons. *Rep. Prog. Phys.* **57**, 1197–1288 (1994).
  - <sup>12</sup> Mertelj, T., Kabanov, V. & Mihailovic, D. Charged Particles on a Two-Dimensional Lattice Subject to Anisotropic Jahn-Teller Interactions. *Phys. Rev. Lett.* **94**, 147003 (2005).
  - <sup>13</sup> Bianconi, A. *et al.* Stripe structure in the  $\text{CuO}_2$  plane of perovskite superconductors. *Phys. Rev. B* **54**, 12018–12021 (1996).
  - <sup>14</sup> Tranquada, J. M., Sternlieb, B. J., Axe, J. D., Nakamura, Y. & Uchida, S. Evidence for stripe correlations of spins and holes in copper oxide superconductors. *Nature* **375**, 561–563 (1995).
  - <sup>15</sup> Kivelson, S. A. *et al.* How to detect fluctuating stripes in the high-temperature superconductors. *Rev. Mod. Phys.* **75**, 1201–1241 (2003).
  - <sup>16</sup> Coslovich, G. *et al.* Ultrafast charge localization in a stripe-phase nickelate. *Nat. Commun.* **4**, 2643 (2013).
  - <sup>17</sup> Sugai, S., Takayanagi, Y. & Hayamizu, N. Phason and Amplitudon in the Charge-Density-Wave Phase of One-Dimensional Charge Stripes in  $\text{La}_{2-x}\text{Sr}_x\text{CuO}_4$ . *Phys. Rev. Lett.* **96**, 137003 (2006).
  - <sup>18</sup> Damascelli, A. & Shen, Z.-X. Angle-resolved photoemission studies of the cuprate superconductors. *Rev. Mod. Phys.* **75**, 473–541 (2003).
  - <sup>19</sup> Schmidt, A. R. *et al.* Electronic structure of the cuprate superconducting and pseudogap phases from spectroscopic imaging STM. *New J. Phys.* **13**, 065014 (2011).
  - <sup>20</sup> Liu, Y. *et al.* Direct Observation of the Coexistence of the Pseudogap and Superconducting Quasiparticles in  $\text{Bi}_2\text{Sr}_2\text{CaCu}_2\text{O}_{8+y}$  by Time-Resolved Optical Spectroscopy. *Phys. Rev. Lett.* **101**, 1–4 (2008).
  - <sup>21</sup> Krasnov, V. M., Yurgens, a., Winkler, D., Delsing, P. & Claeson, T. Evidence for coexistence of the superconducting gap and the pseudogap in Bi-2212 from intrinsic tunneling spectroscopy. *Phys. Rev. Lett.* **84**, 5860–3 (2000).
  - <sup>22</sup> Coslovich, G. *et al.* Competition Between the Pseudogap and Superconducting States of  $\text{Bi}_2\text{Sr}_2\text{Ca}_{0.92}\text{Y}_{0.08}\text{Cu}_2\text{O}_{8+\delta}$  Single Crystals Revealed by Ultrafast Broadband Optical Reflectivity. *Phys. Rev. Lett.* **110**, 107003 (2013).
  - <sup>23</sup> Sacuto, A. *et al.* New insights into the phase diagram of the copper oxide superconductors from electronic Raman scattering. *Rep. Prog. Phys.* **76**, 022502 (2013).
  - <sup>24</sup> Demsar, J., Podobnik, B., Kabanov, V., Wolf, T. & Mihailovic, D. Superconducting Gap  $\Delta_c$ , the Pseudo-

- gap  $\Delta$  p, and Pair Fluctuations above  $T_c$  in Overdoped  $Y_{1-x}Ca_xBa_2Cu_3O_{7-\delta}$  from Femtosecond Time-Domain Spectroscopy. *Phys. Rev. Lett.* **82**, 4918–4921 (1999).
- 25 Kabanov, V. V., Demsar, J., Podobnik, B. & Mihailovic, D. Quasiparticle relaxation dynamics in superconductors with different gap structures: Theory and experiments on  $YBa_2Cu_3O_{7-\delta}$ . *Phys. Rev. B* **59**, 1497–1506 (1999).
  - 26 Madan, I. *et al.* Separating pairing from quantum phase coherence dynamics above the superconducting transition by femtosecond spectroscopy. *Sci. Rep.* **4**, 5656 (2014).
  - 27 Rullier-Albenque, F. *et al.* Nernst Effect and Disorder in the Normal State of High-Tc Cuprates. *Phys. Rev. Lett.* **96**, 2–5 (2006).
  - 28 Li, L. *et al.* Diamagnetism and Cooper pairing above  $T_c$  in cuprates. *Phys. Rev. B* **81**, 1–9 (2010).
  - 29 Alloul, H., Rullier-Albenque, F., Vignolle, B., Colson, D. & Forget, a. Superconducting fluctuations, pseudogap and phase diagram in cuprates. *Europhys. Lett.* **91**, 37005 (2010).
  - 30 Kondo, T. *et al.* Disentangling Cooper-pair formation above the transition temperature from the pseudogap state in the cuprates. *Nat. Phys.* **7**, 21–25 (2010).
  - 31 Toda, Y. *et al.* Quasiparticle relaxation dynamics in underdoped  $Bi_2Sr_2CaCu_2O_{8+\delta}$  by two-color pump-probe spectroscopy. *Phys. Rev. B* **84**, 1–8 (2011).
  - 32 Kusar, P. *et al.* Dynamical Structural Instabilities in  $La_{1.9}Sr_{0.1}CuO_4$  Under Intense Laser Photoexcitation. *J. Supercond. Novel Magn* **24**, 421–425 (2010).
  - 33 Vershinin, M. *et al.* Local ordering in the pseudogap state of the high-Tc superconductor  $Bi_2Sr_2CaCu_2O_{8+\delta}$ . *Science* **303**, 1995–8 (2004).
  - 34 Toda, Y. *et al.* Rotational symmetry breaking in  $Bi_2Sr_2CaCu_2O_{8+\delta}$  probed by polarized femtosecond spectroscopy. *Phys. Rev. B* **90**, 094513 (2014).
  - 35 Yusupov, R. *et al.* Coherent dynamics of macroscopic electronic order through a symmetry breaking transition. *Nat. Phys.* **6**, 681–684 (2010).
  - 36 Kusar, P. *et al.* Coherent trajectory through the normal-to-superconducting transition reveals ultrafast vortex dynamics in a superconductor arXiv:1207.2879.
  - 37 Kusar, P., Demsar, J., Mihailovic, D. & Sugai, S. A systematic study of femtosecond quasiparticle relaxation processes  $La_{2-x}Sr_xCuO_4$ . *Phys. Rev. B* **72**, 014544 (2005).
  - 38 Demsar, J., Hudej, R., Karpinski, J., Kabanov, V. & Mihailovic, D. Quasiparticle dynamics and gap structure in  $HgBa_2Ca_2Cu_3O_{8+\delta}$  investigated with femtosecond spectroscopy. *Phys. Rev. B* **63**, 1–7 (2001).
  - 39 Dvorsek, D. *et al.* Femtosecond quasiparticle relaxation dynamics and probe polarization anisotropy in  $YSr_xB_{2-x}Cu_4O_8$  ( $x=0,0.4$ ). *Phys. Rev. B* **66**, 020510 (2002).
  - 40 Stojchevska, L., Mertelj, T., Chu, J.-H., Fisher, I. R. & Mihailovic, D. Doping dependence of femtosecond quasiparticle relaxation dynamics in  $Ba(Fe,Co)_2As_2$  single crystals: Evidence for normal-state nematic fluctuations. *Phys. Rev. B* **86**, 024519 (2012).
  - 41 Pogrebna, A. *et al.* Spectrally resolved femtosecond reflectivity relaxation dynamics in undoped spin-density wave 122-structure iron-based pnictides. *Phys. Rev. B* **89**, 165131 (2014).
  - 42 Stojchevska, L. *et al.* Electron-phonon coupling and the charge gap of spin-density wave iron-pnictide materials from quasiparticle relaxation dynamics. *Phys. Rev. B* **82**, 1–4 (2010).
  - 43 Gadermaier, C. *et al.* Strain-Induced Enhancement of the Electron Energy Relaxation in Strongly Correlated Superconductors. *Phys. Rev. X* **4**, 011056 (2014).
  - 44 Gay, P., Smith, D. C., Stevens, C. J., Chen, C. & Ryan, J. F. Femtosecond Dynamics of BSCCO-2212. *J. Low Temp. Phys.* **117**, 1025–1029 (1999).
  - 45 Kusar, P. *et al.* Controlled Vaporization of the Superconducting Condensate in Cuprate Superconductors by Femtosecond Photoexcitation. *Phys. Rev. Lett.* **101**, 1–4 (2008).
  - 46 Demsar, J., Forró, L., Berger, H. & Mihailovic, D. Femtosecond snapshots of gap-forming charge-density-wave correlations in quasi-two-dimensional dichalcogenides  $1T-TaS_2$  and  $2H-TaSe_2$ . *Phys. Rev. B* **66**, 041101 (2002).
  - 47 Vishik, I. M. *et al.* Doping-Dependent Nodal Fermi Velocity of the High-Temperature Superconductor  $Bi_2Sr_2CaCu_2O_{8+\delta}$  Revealed Using High-Resolution Angle-Resolved Photoemission Spectroscopy. *Phys. Rev. Lett.* **104**, 207002 (2010).
  - 48 Zhao, G.-m., Hunt, M. B., Keller, H. & Müller, K. A. Evidence for polaronic supercarriers in the copper oxide superconductors  $La_{2-x}Sr_xCuO_4$ . *Nature* **385**, 236–239 (1997).
  - 49 Zhao, G.-m., Conder, K., Keller, H. & Müller, K. A. Oxygen isotope effects in  $La_{2-x}Sr_xCuO_4$ : evidence for polaronic charge carriers and their condensation. *J. Phys. Condens. Mat.* **10**, 9055–9066 (1998).
  - 50 Mihailovic, D., Kabanov, V. V. & Müller, K. A. The attainable superconducting  $T_c$  in a model of phase coherence by percolating. *Europhys. Lett.* **57**, 254–259 (2002).
  - 51 Kohsaka, Y. *et al.* How Cooper pairs vanish approaching the Mott insulator in  $Bi_2Sr_2CaCu_2O_{8+\delta}$ . *Nature* **454**, 1072–8 (2008).
  - 52 Sakai, S. *et al.* Raman-Scattering Measurements and Theory of the Energy-Momentum Spectrum for Underdoped  $Bi_2Sr_2CaCu_2O_{8+\delta}$  Superconductors: Evidence of an s-Wave Structure for the Pseudogap. *Phys. Rev. Lett.* **111**, 107001 (2013).
  - 53 Smallwood, C. L. *et al.* Time- and momentum-resolved gap dynamics in  $Bi_2Sr_2CaCu_2O_{8+\delta}$ . *Phys. Rev. B* **89**, 115126 (2014).
  - 54 In our experiment this component is resolution limited and appear slower. Note that there is another slower component related to thermalization of hot phonons<sup>66</sup>.
  - 55 Kabanov, V. V., Mertelj, T. & Mihailovic, D. Mesoscopic Phase Separation in the Model with Competing Jahn-Teller and Coulomb Interaction. *J. Supercond. Novel Magn* **19**, 67–71 (2006).
  - 56 Mertelj, T., Kabanov, V., Mena, J. & Mihailovic, D. Self-organization of charged particles on a two-dimensional lattice subject to anisotropic Jahn-Teller-type interaction and three-dimensional Coulomb repulsion. *Phys. Rev. B* **76**, 054523 (2007).
  - 57 Keller, H., Bussmann-Holder, A. & Müller, K. A. Jahn-Teller physics and high-Tc superconductivity. *Mater. Today* **11**, 38–46 (2008).
  - 58 Agrestini, S., Saini, N. L., Bianconi, G. & Bianconi, A. The strain of  $CuO_2$  lattice: the second variable for the phase diagram of cuprate perovskites. *J. Phys. A* **36**, 9133–9142 (2003).
  - 59 Mishchenko, A. & Nagaosa, N. Electron-Phonon Coupling and a Polaron in the t-J Model: From the Weak to the Strong Coupling Regime. *Phys. Rev. Lett.* **93**, 036402

- (2004).
- <sup>60</sup> Kivelson, S. A., Fradkin, E. & Emery, V. J. Electronic liquid-crystal phases of a doped Mott insulator. *Nature* **393**, 550–553 (1998).
- <sup>61</sup> He, R.-H. *et al.* From a single-band metal to a high-temperature superconductor via two thermal phase transitions. *Science* **331**, 1579–83 (2011).
- <sup>62</sup> Mook, H. A. & Dogan, F. Charge fluctuations in  $YBa_2Cu_3O_{7-x}$  high-temperature superconductors. *Nature* **401**, 145–147 (1999).
- <sup>63</sup> Mihailovic, D. & Kabanov, V. Finite wave vector Jahn-Teller pairing and superconductivity in the cuprates. *Physical Review B* **63**, 054505 (2001).
- <sup>64</sup> McQueeney, R. J. *et al.* Anomalous Dispersion of LO Phonons in  $La_{1.85}Sr_{0.15}CuO_4$  at Low Temperatures. *Phys. Rev. Lett.* **82**, 628–631 (1999).
- <sup>65</sup> Oda, M. *et al.* Strong pairing interactions in the underdoped region of  $Bi_2Sr_2CaCu_2O_{8+\sigma}$ . *Physica C* **281**, 135–142 (1997).
- <sup>66</sup> Perfetti, L. *et al.* Ultrafast Electron Relaxation in Superconducting  $Bi_2Sr_2CaCu_2O_{8+\delta}$  by Time-Resolved Photoelectron Spectroscopy. *Phys. Rev. Lett.* **99**, 197001 (2007).